Design and fabrication of a micro-optic switch

Wei Li[1, 2], Jingqiu Liang[1,*], Zhongzhu Liang[1] , Xiaoqi Li[1, 2],Weibiao Wang[1], Yanchao Zhong[1, 2], and Degui Sun[3]

[1]State Key Laboratory of Applied Optics, Changchun Institute of Optics, Fine, Mechanics and Physics, Chinese Academy of Sciences, 16 East Nanhu Street,Changchun, JL 130033, China
[2]Graduate School of Chinese Academy of Science, Beijing 100039, China
[3]School of Optoelectrical Enginering, Changchun University of Science and Technology 7089 Weixing Road, Changchun JL 130022, China
[*]Corresponding author:liangjq@ciomp.ac.cn

Abstract: In this paper, a polyimide cantilever micro-optic switch of electromagnetic actuation is studied. The model of the electromagnetic actuation is proposed and simulated using finite element method. The best efficiency of electromagnetic force for switching operations is obtained and the parameters of the coil and magnet are determined. During the practical fabrication, the thick resist patterning and electroplating technology is employed to fabricate the electromagnetic actuation. Both the theoretical and experimental results indicate that the balanceable distance of the polyimide cantilever for implementing optical switches is about 1.28 mm with 0.4 A current pulse input, The final experimental results of optical performance for the fabricated micro-optic 1×4 switch include the switching time of about 20 ms and the insertion loss of about 0.73 dB.

OCIS codes: (130.3120) Integrated optics device; (230.3990) Micro-optical devices; (060.1810) Buffers, couplers, routers, switch, and multiplexers.

References and links

1. C. H. Huang, H. F. Chou, and J. E. Bowers, "Dynamically reconfigurable optical packet switch (DROPS)," Opt. Express **14**, 2008-2014(2006).
2. L. Y. Lin and E. L. Goldstein, "The Roles of MEMS Optical Switches in Fiber-Optic Networks-What and When," Proc. SPIE **5246**, 85-94(2003).
3. H. T. Hsieh, C. W. Chiu, T. Tsao, F. Jiang, and G. D. John Su, "Low-Actuation-Voltage MEMS for 2-D Optical Switches," J. Lightwave Technol. **24**, 4372-4379(2006).
4. C. H. Ko, J. J. Yang, J. C. Chiou, S. C. Chen, and T. H. Kao, "Magnetic Analysis of A Micromachined Magnetic Actuator Using the Finite Element Method," Proc. SPIE **3893**, 127-136(2000).
5. V. G. Kutchoukov, J. R. Mollinger, M. Shikida, and A. Bossche, "Patterning of polyimide and metal in deep trenches," Sens. Actuators A**92**, 208-213(2001).
6. Y. H. Zhang, G. F. Ding, S. Fu, and B. C. Cai, "A fast switching bistable electromagnetic microactuator fabricated by UV-LIGA technology," Mechatronics **17**, 165-171 (2007).
7. J. W. Yang, Y. H. Wu, H. G. Jia, P. Zhang, S. R. Wang, "Design method and magnetic field analysis of axial-magnetized permanent magnet micromotor," Opt. Precision Eng. **14**, 83-88(2006).
8. T. Zhang, Y. H. Wu, H.W. Li, B. Liu, P. Zhang, S. Y. Wang, "Micro electromagnetic actuator with high energy density based on MEMS technology," Opt. Precision Eng. **15**, 866~872(2007).
9. C. T. Pan, and S. C. Shen, "Magnetically actuated bi-directional microactuators with permalloy and Fe/Pt hard magnet," J. Magn. Mag. Matier. **285**, 422-432(2005).

1. Introduction

With the development of optical fiber communication technology, lots of novel optics devices have replaced the traditional electronic ones. All-optical networks have become ubiquitous and formed an irreversible historical trend. Optical switches, including both small switch units and large-scale matrix switches, are the key elements in many optical devices in the all-optical communication systems, e.g., re-configurable optical add/drop multiplexer (ROADM), optical cross connect (OXC) [1], optical switchboard, optical wavelength route etc. The development of optical switches was triggered by rapid predicted growth in the demand for optical

#91827 - $15.00 USD Received 17 Jan 2008; revised 16 Mar 2008; accepted 2 Apr 2008; published 21 Apr 2008

networks, combined with the maturation of micro-electrical mechanical system (MEMS) technology. Compared to other optical switches that have been previously developed, the MEMS optical switches not only have the advantages of small volume, light weight, low power consumption and easy integration, but also bear the outstanding characteristics of free-space optical propagation to implement bit-rate transparency, route selection, OXC switching and add /drop optical signals in the ROADM systems [2, 3].

An electromagnetic (EM) optical switch was designed in this study. Compared to other types of drive, e.g., electrostatic drive, shape memory alloys drive, thermal drive and piezoelectric drive etc, the main advantage in using an EM principle for actuation is the capability of providing higher force over larger distance [4]. Some parameters of the coil and the magnet were designed and simulated. The thick photo-resist patterning of AZ4903 and the electroplating technology was used to fabricate the planar coil. The performance of the optical switch was measured. This paper is certainly valuable to the application and development of the all-optical networks.

2. Design and theoretical analysis

The EM optical switch based on polyimide cantilever was designed using polyimide via its excellent properties of good insulation, high mechanical intensity, good heat-endurance and strong impregnant-endurance [5]. A schematic structure of the micro-optic 1×N switch with an EM actuation is shown in Fig. 1 (here N=2). The optical switch consists of a substrate holding N switching ports, and at each switching port there are a permanent magnet, a copper coil, a polyimide cantilever and a beam steaming prism. The permanent magnet is used to hold the polyimide cantilever together with the coil and the beam steaming prism at a desired lifted position by means of the fluxes in the air gap. As depicted in Fig. 1, if no switching port is required to have an output of optical beam, the input optical beam can directly go out without any blocking, while if one switching port is required to have an output of the optical beam, the coil is activated and a magnetic force make the polyimide cantilever together with the coil and the beam steaming prism go down to the blocking position of optical beam path and the prism deflects the optical beam go out from the output port. To integrate the optical switch into MEMS, all the coils are designed in planar structure. The fluxes of magnet can be regulated by the planar coil fed into the electric current with a certain direction. The change of flux density in the air gap leads to a resultant force exerting on the polyimide cantilever lift or fall the beam steaming prism. The aforementioned process is the operating principle of the 1×N optical switches studied in this work. In fact, this 1×N optical switch is composed of optical beam paths connected with one input port and N outputs on a MEMS substrate, and N actuators corresponding to N output optical beam paths. Each actuator is composed of a polyimide cantilever and a coil to for lifting a beam steering prism.

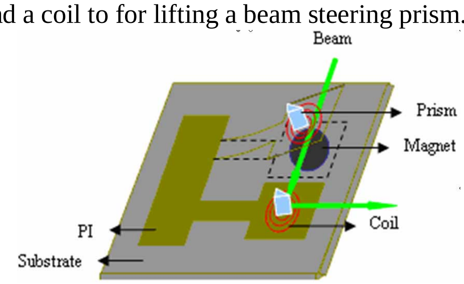

Fig. 1. Schematic structure of the micro-optic switch of EM actuation.

The actuation principle is based on the resultant EM force resulted from the fluxes of magnet through the air gap. The EM force is calculated and designed from the following equation [6]:

$$F = \frac{1}{2\mu_0 S}\Phi^2 \tag{1}$$

#91827 - $15.00 USD Received 17 Jan 2008; revised 16 Mar 2008; accepted 2 Apr 2008; published 21 Apr 2008

Where μ_0 and S are the permeability and the section area of the air gap, respectively; Φ is the resultant fluxes.

In order to obtain the insight of the mechanism, the magnetic problem was analyzed using the finite element software [7]. The parameters of the device are defined as follows: the coil width *w*, the coil thickness *t*, the distance *wd* between two adjacent coils, the magnetic radius *r*, the magnetic height *h*, the distance *d* between coil and magnet (air). The coil's material is Cu by assuming the effective permeability $\mu = 1$. The magnetic material block is made by NdFeB with an effective permeability $\mu = 4$. For the reason of axial symmetry of the planar coil and magnet, only half of the device here was modeled (Fig. 2). Figure 3 shows the magnetic density *B* by the planar coil and magnet. Note that there exists a maximum magnetic density 0.83 T. The simulated results indicate that the force between the planar coil and magnet is about 1.69 mN.

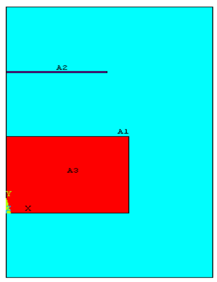

Fig. 2. Two-dimention axis-symmetrical section model of the coil and magnet.

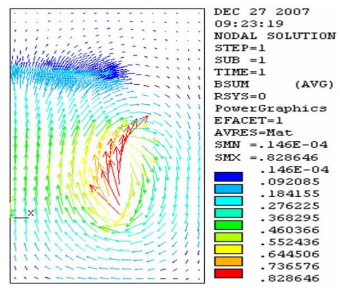

Fig. 3. Magnetic flux of the EM actuation.

The increase of the coil's numbers and section area can generate a relatively large EM force under the condition of the finite area. Therefore, it is crucial to design the numbers and section area of the coil. However, the numbers of the coil can not increase infinitely and the increase of the section area needs the increase of the coil width or thickness, but the increase of the width brings to the reduction of the coil's numbers.

The EM force between the permanent magnet and the coil is defined as following equation [8]：

$$F_z = \int_V \frac{d(M \bullet B_z)}{d_z} dV = MV \frac{\partial B_z}{\partial z} \tag{2}$$

Where *M* is the magnetization, *V* is the volume of the magnet, B_z is the magnetic flux density produced by the coil in the vertical direction and $\partial B_z / \partial z$ is the gradient of the magnetic field. Equation (2) indicates that F_z is proportional to $\partial B_z / \partial z$ or *V*. Furthermore, it can be inferred that B_z is axis-symmetrical. To optimize the magnetic performance, the magnet should be in place. The main advantage of the magnet under the coil is the EM force can increase rapidly with the increase of the magnetic volume, which can be seen in equation (2).

There are two ways to increase EM force with the fixed numbers of the coil:

1) The resistance *R* of the planar coil is inversely proportional to *wt* which is the cross-section area of the planar coil line. The thicker planar coil can reduce the value of *R*, by which the input voltage and current can generate a larger magnetic force output.

$$R = \rho \frac{l}{wt} \tag{3}$$

Where ρ is resistivity of coil material, *l*, *w* and *t* are the length, width, and thickness of the planar coil, respectively. With equations (2) and (3), the relation between the EM force and the coil thickness *t* as depicted in Fig. 4. It is obvious that the EM force is linearly

#91827 - $15.00 USD Received 17 Jan 2008; revised 16 Mar 2008; accepted 2 Apr 2008; published 21 Apr 2008

increased as the thickness of the coil increases under the condition of the same current density.

2) The simulation for the EM force versus the width of coil shows that the EM actuation with high aspect ratio planar coil could similarly sustain higher electric current that consequently increases the EM force, as shown in Fig. 5, which is also a linear relation between the EM force and the width of the coil.

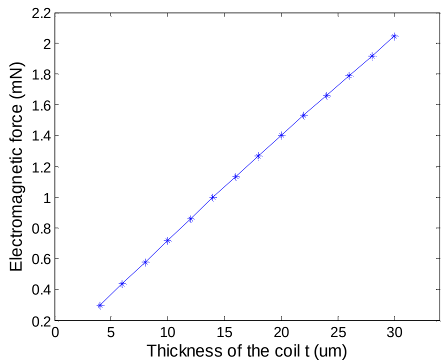

Fig. 4. EM force versus the thickness of the coil.

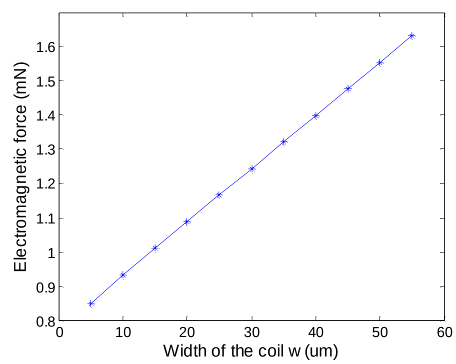

Fig. 5. EM force versus the width of the coil.

During the fabrication of realistic devices, the coil parameters should be selected flexibly according to the experimental conditions and the demand of the device. Here, the width of the coil w is 48 µm, the distance between two adjacent coil lines w_d is 12 µm, the thickness of the coil t is 20 µm, and the outer radius of the coil r_c is 1.2 mm.

To extract the parameters of the EM optical switch, the relations between the height of magnet h, the radius of magnet r and the resulting EM force were studied. Assuming that r is 1.2 mm, the distance d between the planar coil and magnet is 1 mm and the current is 0.2 A, the numerical simulation results of the EM force versus h are obtained as shown in Fig. 6. Note that the EM force is increased with the increase of h, but the slope of the curve decreases slowly. This implies the value of the EM force is radically affected by h and the EM force is gradually approaching a stable value when h is greater than 3 mm. So h is determined flexibly by the dimension and the demand of the device. Similarly, the change of the EM force versus r with respect to h is studied and the results for the two cases are obtained as shown in Fig. 7. Note that for the case that h is 1.2 mm, when r is in the range from 0 to 1.45 mm, the EM force increases linearly, and when r is greater than 1.45 mm, the EM force decreases slowly, so it has reached the maximum value of 1.69 mN at r=1.45 mm. For the case that h is 3.0 mm, the EM force has reached the maximum value of 2.28 mN at r=1.62 mm.Thus, it turns out that the value of h not only determines the maximum value of EM force, but it also affects the

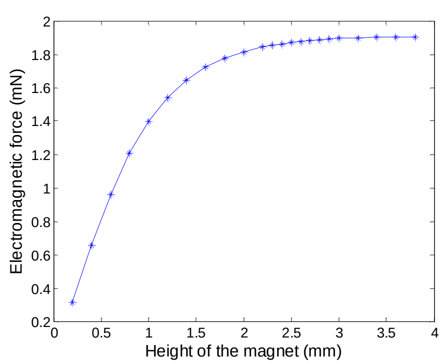

Fig. 6. EM force versus the height of the magnet.

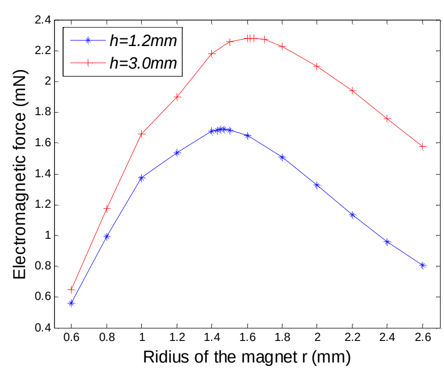

Fig. 7. EM force versus the radius of the magnet.

#91827 - $15.00 USD Received 17 Jan 2008; revised 16 Mar 2008; accepted 2 Apr 2008; published 21 Apr 2008

corresponding value of *r*. The height *h* is determined by considering the required EM force which can satisfy natural work of the device and the smaller volume of the device. The higher magnet is better if the volume of the device is not strict. The simulation of the magnet has been completed and the optimal parameters in this study are: *h* is 1.2 mm and *r* is 1.45 mm.

For the case that the current is 0.4 A, the *h* is 1.2 mm and *r* is 1.45 mm, the numerical simulation curve of the EM force versus the distance *d* between the magnet and coil is shown in Fig. 8. Note that the EM force decreases with the increase of *d*, the relation between the force and *d* is linear when *d* is in the range between 0.2 mm and 0.6 mm. However, the force decreases slowly when *d* is greater than 0.6 mm. Similarly, the change of EM force with the given *d* (*d*=1 mm) is observed by varying the current and the results are shown in Fig. 9. Note from Fig. 9 that the force linearly increases with the increase of the current.

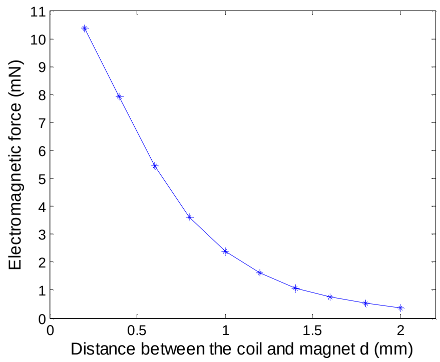

Fig. 8. EM force versus the distance between the coil and magnet.

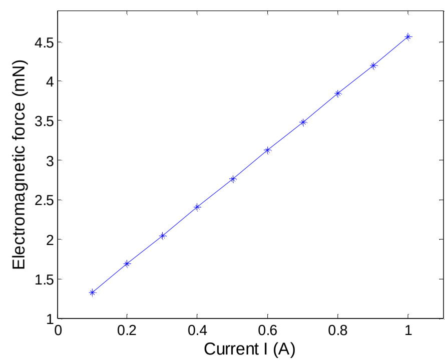

Fig. 9. EM force versus the current.

3. Fabrication Technology and Experimental Results

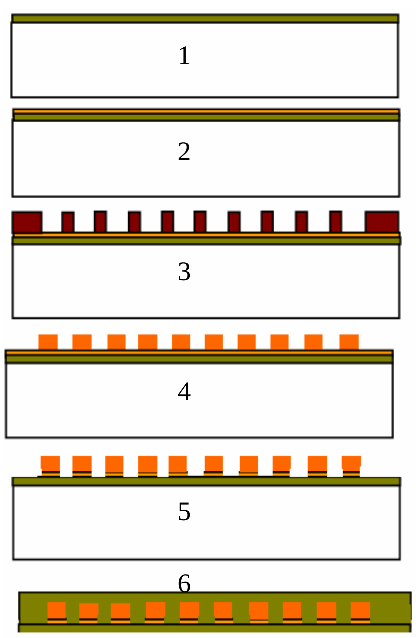

Fig. 10. Processing program for fabricating the PI cantilevers and the planar coils for the EM micro-optic switch.

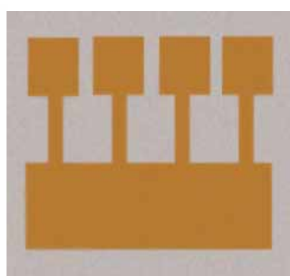

Fig. 11. Top-view structure of the polyimide cantilever.

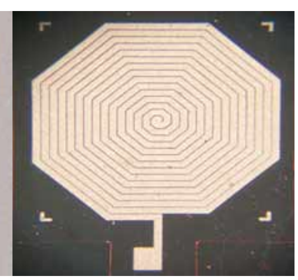

Fig. 12. Photo-picture of the planar coil after electro-plating.

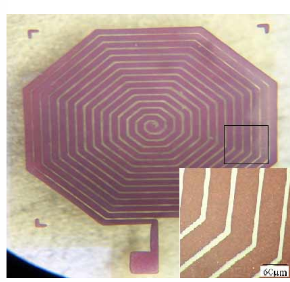

Fig. 13. Photo-picture of the planar coil after etching.

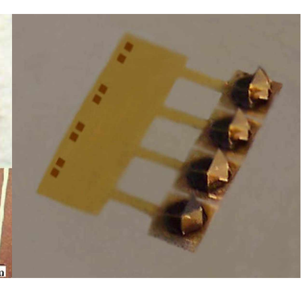

Fig. 14 Photo-picture of the fabricated optical switch.

#91827 - $15.00 USD Received 17 Jan 2008; revised 16 Mar 2008; accepted 2 Apr 2008; published 21 Apr 2008

An efficient processing program for the fabrication of the polyimide cantilevers and coils was developed as shown in Fig. 10 [9]. Basically there were six stages in the program. (1) A polyimide layer was spin-coated on a silicon wafer and baked on the wafer that was used to fabricate polyimide cantilever, (2) a resist BP218 layer was spin-coated, exposed with the mask of cantilevers (Fig. 11), and developed and then a Cu seed layer with 200 nm thickness for electroplating was sputtered after a polyimide cantilever layer was deep baked, (3) a thick AZ4903 resist layer with 30 μm thickness was spin-coated, exposed with the mask of coils, and developed, (4) a thick Cu layer was electroplated on the given pattern (Fig. 12), (5) the resist layer was stripped and the Cu seed layer was etched to form the coils (Fig. 13), and (6) the polyimide layer was spin-coated on the final pattern that acted as an insulating and protecting layer. Then the wafer was removed and the structure of the polyimide cantilevers and coils was finished. Finally, the structure of the polyimide cantilevers and coils was fixed on the substrate having magnets. This process requires that the coil position and the magnet position must be opposite to each other. The coil is about 50 μm in width, 10 μm in gap, 23 μm in thickness and 2 Ω in resistance. After all the prisms were pasted on the cantilevers, a 1×N (N=2, 4, or 8) electro-magnetic switch was formed. The photo-picture of the fabricated 1×4 optical switch is shown in Fig. 14.

Upon the simulation and manufacturing have been completed, a series of experiments were performed on the optical switch. In order to measure the curvature or the deformation of the polyimide under the effect of the EM force, a schematic diagram for measuring the lifting performance of the cantilevers in the experimental devices is shown in Fig. 15(a), where the weight of the prism is neglected because the prism is light, the alternating current was applied onto the experimental devices and the signals were recorded into computer via a data collection card. For the best case of the EM force with the optimal parameters of the cantilevers: I=0.4A, h=1.2 mm and r=1.45 mm, which were obtained in Section 2 as depicted in Fig. 8, the results of the data processing depicted in Fig. 16 indicate the relation between the lifting height (or displacement of cantilever) and drive current, where the simulation results and measured data are compared. Note that the lifting height of the cantilever increases with the increase of the current and the experimental data are almost in line with the simulation results, which imply that the method of MEMS EM optical switch's design is feasible. Further note from Fig. 16 that the lifting distance of cantilevers is over 1.28 mm when electric current I=0.4 A, which is sufficient for an optical beam to pass through. This lifting distance is referred to as balanceable distance of the polyimide cantilever. As the second stage of experiments, a schematic diagram for measuring the switching operations of the experimental devices is shown in Fig. 15(b), an optical signal was emitted by steady laser when a drive current was put on the coil, then the cantilever with the coil and prism sway up and down under the EM force induced by the drive current and finally the propagation direction of the optical signal was changed by the reflecting prism. If we make one of N outputs export the optical signal the output of optical signal can be received, so a complete 1×N EM micro-optic switch can be implemented. In this process, the wave of the optical signal via the optical-electrical (O-E) conversion is observed by the oscilloscope, which

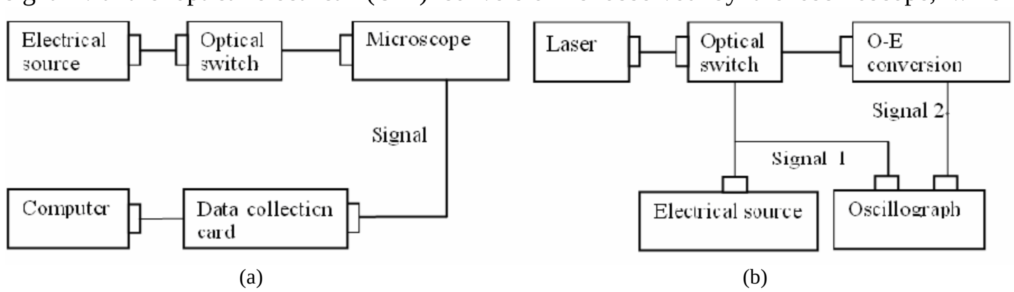

Fig. 15. Schematic diagram of the experiment devices: (a) measuring displacement; (b) measuring response time

#91827 - $15.00 USD Received 17 Jan 2008; revised 16 Mar 2008; accepted 2 Apr 2008; published 21 Apr 2008

indicates that the response time of the optical switch is about 20 ms. The insert-loss of the optical switch is about 0.73 dB. When the current of the coil is about 1.1 A, the coil was burned down due to the high temperature produced by Joule's law. So the working current of the coil should be controlled much less than 1.1 A to protect the coil.

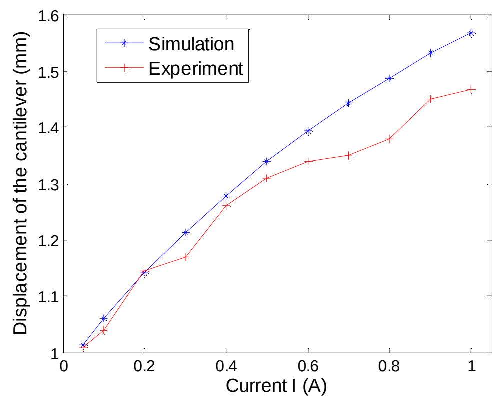

Fig. 16. Displacement of the cantilever versus the current.

4. Conclusion

An EM micro-optic switch is studied and demonstrated in this paper. The results of numerical simulation from finite element method indicate that the dimension of the coil and magnet have great influence on the EM force. The EM force increases dramatically with the increase of the coil's thickness or aspect ratio. Furthermore, the best efficiency in the electromagnetic force is obtained when the current I is 0.4 A, the height h of magnet is 1.2 mm and the radius of magnet r is 1.45 mm, at which the polyimide cantilever can produce a balanceable distance of 1.28 mm. During the fabrication for the realistic experimental devices, the thick resist patterning and the electroplating technology was employed to improve the efficiency and performance of the EM optical switch. Experimental results verify the usefulness of the guidelines obtained from simulations. The MEMS-based EM optical switch can be used in wave-division-multiplexer (WDM) system or micro-optic system as either wavelength selective switches or a direct dropping device of optical wavelength signal from the WDM data flow of WDM fiber-optic communication systems. The regime of EM optical switches has shown a significant essence of applications in both modern and future optical networks and other information systems because of the advantages of small volume, light weight, low power consumption and easy integration.

Acknowledgments

This work is performed with support from the National Natural Science Foundation of China (No: 60578036) and Scientific Research Startup Foundation for excellent thesis for doctor's degree and the gainer of prior award. The authors would like to thank Yanmei Kong doctor for helpful discussions on the theory and experimental setup.